PRS GLOBAL OPEN

ORIGINAL ARTICLE

Research

Effect of Photobiomodulation With Different Wavelengths on Radiodermatitis Treatment

Cristina Pires Camargo, MD, PhD*
Arturo Forner-Cordero, PhD†
Bruna Matsumoto Silva, BEng‡
Vinícius Melo de Souza, BEng‡
Higor Souza Cunha, BEng‡
Yasmin de Oliveira Feitosa, BEng‡
Guilherme Arellano Campello, BEng‡
Pedro Henrique Gianjoppe dos Santos, BEng‡
Carolina Logo Rego, BEng‡
Heloisa Carvalho, MD, PhD§
Rolf Gemperli, MD, PhD*

Background: Approximately 80% of patients submitted to radiotherapy develop radiodermatitis. Photobiomodulation based on light-emitted diode (LED) is one of the therapeutic strategies for treating inflammation. This study aimed to investigate the effect of the photobiomodulation with two wavelengths, in an acute radiodermatitis animal model.

Methods: Twenty rats were submitted to one radiotherapy session. After 15 days, the rats that developed radiodermatitis were divided into control groups, LED-630 nm, LED-850 nm, and LED-630+850 nm. The treatment regimen was one session lasting 10 minutes on alternate days for 21 days. We analyzed macroscopy aspects (RTOG scale), vascular density, dermal appendages, VEGF-a, TNF-alpha, MMP-9, and MMP-9 genic expression level.

Results: All LED groups revealed a two-point reduction on the radiodermatitis severity grade compared with the baseline classification. Dermal appendage and vascular analysis showed a higher counting in all LED groups compared to control. This study showed dermal appendages twice in the 630/850 nm group compared with the control group. The 630/850 nm group showed six times more arterioles than the control group. Regarding genic expression, this study showed a 10-fold decrease between LED-630 nm versus LED-630+850 nm ($P = 0.02$) interleukin-10 expression and a 12-fold decrease between control versus LED-630 nm ($P = 0.006$) and LED-850 nm ($P = 0.002$) in TNF-alpha.

Conclusion: LED (630 nm, 850 nm, and 630 nm + 850 nm) showed benefit in the treatment of radiodermatitis, and the association of the 630 nm + 850 nm and 630 nm parameters demonstrated the best macroscopic and microscopic results. *(Plast Reconstr Surg Glob Open 2023; 11:e4809; doi: 10.1097/GOX.0000000000004809; Published online 2 February 2023.)*

INTRODUCTION

Radiotherapy is an adjuvant treatment in oncology. More than 50% of cancer patients will receive irradiation for a curative or palliative purpose.[1–3] Radiotherapy is mostly delivered by radiation equipment (external beam radiation). Radiotherapy equipment emits high-energy particles or waves in the target organ that penetrate and exit the body through the skin.

The mechanism of action of radiotherapy treatment, as an ionizing radiation, generates indiscriminate DNA breakdown in malignant and normal cells. DNA damage precludes the process of cell repair and consequently induces apoptosis. Depending on the magnitude of cell injury, the level of tissue damage, and thus the radiodermatitis, will vary.[1,2] However, an important negative effect is that approximately 85%–90% of patients submitted to radiotherapy will develop radiodermatitis.[4]

Disclosure: *The authors have no financial interest to declare in relation to the content of this article.*

Several factors could contribute to radiodermatitis severity: radiation dose and administration protocol; comorbidities; smoking; associated treatments, for example, use of chemotherapy; and patient skin sensitivity.[2] Symptoms in the irradiated area range from mild local burning sensation to skin ulcerations. In addition, radiodermatitis can be classified according to the time of onset of the signs in acute (first 90 days after irradiation) or chronic (months and years after irradiation).[1,5,6]

For mild-to-moderate radiodermatitis, routine clinical treatment consists of topical agents (moisturizing creams, lotions, and topical corticosteroids). For severe radiodermatitis, systemic agents (corticosteroids and antioxidants) can be used.[6,7] However, the effectiveness of the available treatments is unpredictable. Moreover, here is no consensus on which of these therapeutic approaches would be more effective in treating radiodermatitis.[6,7]

It must be taken into account that radiodermatitis can negatively affect the patient's quality of life due to painful irradiation lesions.[2] Recently, several authors analyzed the use of low-level laser therapy (LLLT), also known as photobiomodulation (PBM), for radiodermatitis treatment.[8–11] PBM activates mitochondria membrane acceptors by cytochrome C oxidase enzyme activation. The cytochrome C oxidase enzyme is present in the electron transport chain, and this enzyme is fundamental for life-supporting function of adenosine triphosphate (ATP) synthesis in the mitochondria.[10]

Studies have shown that this molecule acts as a photoacceptor and transducer of photosignals at the red and infrared light spectrum wavelengths. The acceptor's stimulus increases the transport of electrons in the mitochondria membrane, and consequently, increases the production of ATP in the mitochondria.[10,11]

More than 50% of cancer patients will receive irradiation for a curative or palliative purpose.[1–3] The mechanism of action of radiotherapy treatment, as ionizing radiation, generates indiscriminate DNA breakdown in malignant and normal cells. DNA damage precludes the process of cell repair and consequently induces apoptosis. Approximately 85%–90% of patients submitted to radiotherapy will develop any radiation skin injury (radiodermatitis).[4]

Several factors could contribute to radiodermatitis severity: radiation dose and administration protocol, comorbidities, smoking, associated treatments (for example, the use of chemotherapy), and patient skin sensitivity.[2] The symptoms in the irradiated area range from a mild local burning sensation to skin ulcerations.[1,5,6]

Routine clinical treatment consists of topical agents (moisturizing creams, lotions, and corticosteroids) for mild-to-moderate radiodermatitis. For severe radiodermatitis, systemic agents (corticosteroids and antioxidants) can be used.[6,7] However, the effectiveness of the available treatments is unpredictable, with no clinical consensus.[6,7] In addition, depending on the magnitude of radiodermatitis, the symptoms can impact the patient's quality of life.[2]

Recently, several authors analyzed the use of LLLT for radiodermatitis PBM treatment.[8–11] PBM activates

Takeaways

Question: Can photomodulation treat radiodermatitis?

Findings: LED (630 nm, 850 nm, and 630 nm + 850 nm) showed benefit in the treatment of radiodermatitis, and the association of the 630 nm + 850 nm and 630 nm parameters demonstrated the best macro and microscopic results.

Meaning: This study suggested photomodulation treatment is an alternative for radiodermatitis treatment in an animal model.

mitochondrial membrane acceptors by cytochrome C oxidase enzyme activation. The cytochrome C oxidase enzyme is present in the electron transport chain. This enzyme is fundamental for the life-supporting function of ATP synthesis in the mitochondria.[10]

Studies have shown that this molecule acts as a photoacceptor and transducer of photosignals in the red and infrared light spectrums. The acceptor's stimulus increases the transport of electrons in the mitochondrial membrane. Consequently, electron movement increases the production of ATP in the mitochondria.[10,11]

In several studies, PBM therapy showed significant efficacy in preventing radiodermatitis from breast cancer. But some questions remain open about the effects of PBM in radiodermatitis treatment.[8,9]

For instance, there is no consensus on the light source and its parameters (wavelength, irradiance, and fluency). Some studies showed a benefit of using wavelengths between 600 and 700 nm for superficial tissue and between 780 and 1000 nm for deeper tissues.[9,10]

Also, there is no data regarding the source of light's physical effect or the interaction between light and molecules and tissues. From the physiological point of view, the absorption of low-intensity light by the biological system is not constant, as is the light emitted by the light-emitting diode (LED).[10] Some papers in the literature show a benefit of using 630 nm (red), while other authors indicate better results using 850 nm (infrared). However, it is not clear from the literature whether therapy with a combination of wavelength(s) may yield better radiodermatitis recovery. Thus, we hypothesize that a variety of two wavelengths could provide better results due to the complementary effects of each wavelength on dermatitis. To perform this experimental study, we developed low-cost LED equipment for PBM that allows the application of these wavelengths. Thus, this study analyzed the effects of PBM with different wavelengths for treating acute radiodermatitis in rats submitted to ionizing radiation as a preliminary step to clinical testing.

METHODS

We analyzed 20 male Wistar rats with weight ranging from 200 to 250 g. The study followed the national standards of best practices in animal care according to CONCEA (Conselho Nacional de Controle de Experimentação Animal) guidelines and was approved by

CEUA-FMUSP (Comissão de Ética no Uso de Animais), School of Medicine da Universida de São Paulo under registration 1060/2018. We followed ARRIVE (Animal Research: Reporting of In Vivo Experiments) guidelines for animal experiments.

Radiodermatitis Induction and Assessment

All rats were anesthetized by an intraperitoneal injection of the association of ketamine hydrochloride (Ketamin, Cristália, Brasil) 100 mg/kg and xylazine hydrochloride (Rompun, Bayer, Brasil) 5 mg/kg. All rats were placed in dorsal decubitus, and an area of 10×6 cm in the back of the animal was trichotomized. Radiation was delivered with two Strontium-90 (^{90}Sr) dermatological plaques that emit beta radiation (Model SIQ21, with reference dose rate = 0.051 Gy/s and Model SIQ18 with reference dose rate = 0.048 Gy/s, Amersham International plc). Two areas of 2×2 cm on the dorsum of each animal were exposed to a single dose of 20 Gy. The areas were at least 3 cm apart.[8–10]

The animals were then kept in a vivarium for 15 days until the appearance of radiodermatitis lesions. After this period, they were divided into four groups:

- Control Group: n = 5, no further treatment
- Group LED, 630 nm: n = 5, exposure to LED, one session lasting 10 minutes on alternate days, for the following 21 days.
- Group LED, 850 nm: n = 5, exposure to LED, one session lasting 10 minutes on alternate days, for the following 21 days.
- Group LED, 630 nm + 850 nm: n = 5, exposure to LED, one session lasting 10 minutes on alternate days, for the following 21 days.

Development of LED Equipment

The development of the LED photoemitter equipment was performed by Grupo ARGO—an interdisciplinary undergraduate team from USP dedicated to biomedical engineering and health innovation. Such device allows sessions from 1 to 30 minutes with red (630 nm) LEDs, infrared (850 nm) LEDs, or both simultaneously. The equipment allows the operator to customize the treatment session, by adjusting the irradiance of the incident light on the injury and selecting the wavelength to be used.

Table 1. Correspondence between Wavelength (nm), Light Irradiance (W/cm²), Light Fluency (W/cm²), and Exposure Time (s)

Wavelength (nm)	Irradiance Scale	Irradiance (W/cm²)	Exposure Time (Seconds)	Light Fluency (J/cm²)
630	Minimum	0.009	360	3.24
850	Minimum	0.016	360	5.76

The device enables the operator to choose among three distinct values of irradiance ("maximum," "medium" and "minimum"), which is a measurement of the amount of energy per unit time that reaches a certain area, and three different emitted wavelengths (630 nm, 850 nm, and both at the same time), and the time of light exposure. Table 1 describes the correspondence between the choices and irradiance (in W/cm²) reaching the animal's injury. For the tests performed on the rats, the red-light fluency obtained was 3.24 J/cm², and the infrared light fluency was 5.76 J/cm² with 6 minutes for each test (Table 1).

All irradiance measurements were made with Model 1825-C Power/Energy Meter from Newport and the sensor 818-SL/DB silicon (Si) photodetector. The electronic part of the device is responsible for controlling both the wavelength emitted by the LEDs and the irradiance (W/cm²) of light applied to the animal's injury. We used the circuit schematically depicted in Figure 1, comprising five infrared LEDs (850 nm), 36 red LEDs (630 nm), TIP-122 transistors, varied SMD resistors, 4.3-inch Nextion NX4827T043, and ATmega328 microcontroller.

Macroscopic Analysis of Radiodermatitis

After the 15th postirradiation day and on the 21st day of treatment with LED, the dorsal region of the animals was photographed (Canon EOS Rebel T7 DSLR, 24.1 MP, Canon). Two independent investigators analyzed the dorsal skin area before the 15th postradiotherapy session and every week during the 3 weeks of treatment, and reactions were classified using the RTOG scale (Table 2).[12]

Microscopic Analysis

At the end of 21 days after group assignment, the animals were killed by an intraperitoneal injection of the combination of ketamine hydrochloride (Ketamin, Cristália,
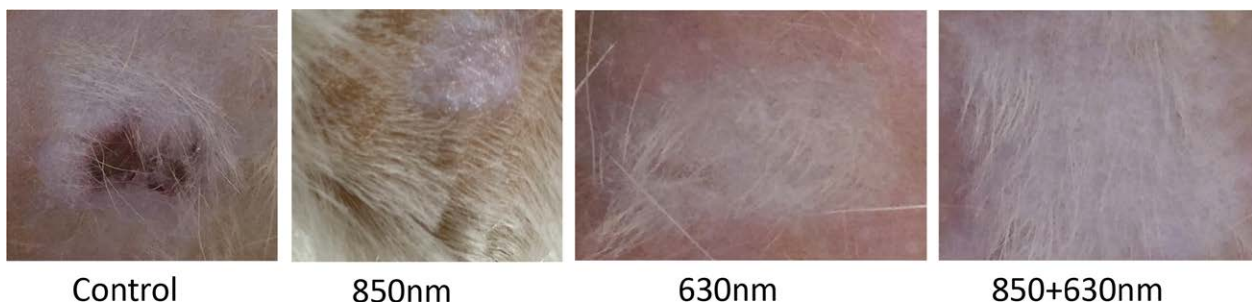

Fig. 1. Macroscopic view after treatment. The first row is the pretreatment lesions. The second row is after 21st day of treatment with LED. Each column corresponds to control group, 850 nm group, 630 nm group, and 850 + 630 nm group.

Control   850nm   630nm   850+630nm

Table 2. RTOG Scale

Histological Structures	Control Median (IQR); 95% CI	630 nm Median (IQR); 95% CI	850 nm Median (IQR); 95% CI	630/850 nm Median (IQR); 95% CI
Dermal appendages	16.5 (15–20); 14.4–18.9	21 (17–24); 17.9–24.0	10.5 (8–12); 8.1–13.3	34.5 (30–42); 1.1–1.8
Arterioles	4.5 (3–8); 3.2–5.8	5 (3–6); 3.1–7.6	4 (3–6); 1.9–5.8	26 (19–29); 6.4–13.8

Grade 0: normal appearance.
Grade 1: minimal erythema, decreasing sweating.
Grade 2: tender or bright erythema, patchy moist desquamation, and moderate edema.
Grade 3: erythema associated with confluent dry desquamation, edema.
Grade 4: ulceration, hemorrage, and necrosis.
Grade 5: necrosis.
Adapted from the work by Cox et al.[12]

Brasil) 150 mg/kg and xylazine hydrochloride (Rompun, Bayer, Brasil) 10 mg/kg. Two samples from each lesion were collected. One was prepared for histological analysis, and the other was frozen with nitrogen −80°C to perform interleukin-10 (IL-10) and matrix metalloproteinase-9 (MMP-9) analysis.

One sample was fixed in 4% formalin for 24 hours, embedded in paraffin for hematoxylin-eosin and picrosirius staining. After hematoxylin-eosin staining and under optical microscopy (Nikon eclipse E600, Japan) magnification (20× and 40×), we quantified the vascular density (angiogenesis) and dermic appendages (number of hair follicle). Picrosirius staining was used to assess collagen fiber distribution and density (graphic distribution structure). We analyzed and quantified all the above histological structures in 10 fields per slide. A blinded investigator performed the analysis of all the samples.

ANALYSIS OF GENE EXPRESSION (IL-10, TNF-ALPHA, VEGF-A, AND MMP-9)

Total RNA Extraction

The samples of fleshy panicle were macerated using the Tissue Lyser LT apparatus (Qiagen, Germantown). 1.0 mL of Trizol (Invitrogen-Life Technologies, Carlsbad) and stainless-steel beads were added to the microcentrifuge tubes. Fragmentation was performed for 6 minutes at 50 Hz.

After removing the beads, 0.2 mL of chloroform (Merck) was added. The samples were centrifuged for 15 minutes at 12,000 rpm at 4°C. After centrifugation, the aqueous phase was transferred to a new microcentrifuge tube, and 0.5 mL of cold isopropyl alcohol (Merck) was added to precipitate the RNA. The samples were incubated at room temperature for 10 minutes and then centrifuged at 12,000 rpm for 10 minutes at 4 °C. The supernatant was discarded, and the precipitate, containing RNA, was washed with 1.0 mL of 75% ethanol. It was centrifuged for 5 minutes at 10,000 rpm at 4°C. The flask containing RNA was resuspended in 50–100 μL of sterile ultrapure water free of DNase/RNase (Invitrogen-Life Technologies, Carlsbad).

The concentration of the extracted RNA was determined on a NanoDrop ND-1000 spectrophotometer (NanoDrop Technologies, Inc., Wilmington). The degree of purity was evaluated by the ratio 260/280 nm, using only RNA with a ratio greater than or equal to 1.8. For the analysis of the integrity of the RNA, electrophoresis in agarose gel was performed to check the 28S and 18S bands. The extracted RNA was stored at −80 °C until use. The degree of purity of the RNA was confirmed with the average ratio greater than or equal to 1.9.

Synthesis of cDNA

For the synthesis of cDNA, from the total RNA, the High-Capacity RNA-to-cDNA kit (Applied Biosystems) was used in a GeneAmp 2400 thermocycler (Applied Biosystems). The probes and primers for the genes and for the endogenous control were purchased from Applied Biosystems. Real-time polymerase chain reaction (qRT-PCR) was performed in duplicate for each sample using 10.0 μL TaqMan Universal Master Mix II 2X, 1 μL TaqMan Gene Expression Assay 20X, and 4 μL diluted cDNA (1:5 dilution) for a final volume of 20 μL in 96-well plates coated with optical sealant. The reaction conditions were 50°C for 2 minutes, 95°C for 10 minutes, 40 cycles at 95°C for 15 seconds, and 60°C for 1 minute.

Real-Time Polymerase Chain Reaction

The analysis of gene expression of the mRNA levels of interest was performed by qRT-PCR in the StepOnePlusTM thermocycler (Applied Biosystems) with the TaqMan Gene Expression Assays system (Applied Biosystems). The probes and primers for the C5AR1 (Rn02134203), ICAM 1 (Rn 00564227), iNOS (Rn 00561646), VEGF (Rn 01511602), and for the endogenous control ACTB (Rn 00667869) were acquired from the company's list of inventoried assays Applied Biosystems. QRT-PCR was performed in duplicate for each sample using: 10.0 μL TaqMan Universal Master Mix II 2X, 1 μL TaqMan Gene Expression Assay 20X, and 4 μL of diluted cDNA (dilution 1: 5) in a final volume of 20 μL, in 96-well plates covered with optical sealant.

Reaction conditions were as follows: temperature of 50°C for 2 minutes, 95 °C for 10 minutes, followed by 40°C cycles at 95°C for 15 seconds and 60°C for 1 minute. To calculate the expression level of each target gene, we used the GenEx Standard 6.1 software (MultiD Analyzes AB), which employs the $2^{-\Delta\Delta C_t}$ method for relative quantification, where C_t (threshold cycle) is the real-time PCR, in which the amplification reaches the logarithmic phase, where delta Ct is the difference in expression between the target gene and endogenous control of a given sample and $2^{-\Delta\Delta C_t}$ values corresponds to the difference between the $2^{-\Delta\Delta C_t}$ of the sample and the $2^{-\Delta\Delta C_t}\theta$ of control.

Statistical Analysis

Because of the small sample size, the variables of the four groups were compared using the Kruskal-Wallis test (nonnormal distribution). If a significant difference was found, a post hoc test (Dunn test) was performed. We considered an alpha of 0.05 and 80% power. Statistical software STATA version 14 (StataCorp. 2015. Stata Statistical Software: Release 14. College Station, TX: StataCorp LP) was used for calculation.

RESULTS

In this study, there were no animal losses.

Macroscopic Analysis

On day zero of the LED treatment, the animals were classified according to the radiodermatitis scale as grade 5. After the 21st day of treatment with LED with the different wavelengths of all exposed groups (630 nm, 850 nm, and 630/850 nm), the radiodermatitis severity was reduced to grade 2. In the control group, radiodermatitis scores were the same as baseline, as presented in Figure 1.

Microscopic Analysis

The control group presented no organized epidermis (less basaloid cells and more keratin). The group exposed to 630 nm and 850 nm showed that all the epidermic layers intact, but keratin structure was missing when compared to the control group, with basal cells migrating from basal to superficial layers.

The 630/850 nm group showed an intact epidermis, with organized formation of the layers and signs of early keratinization.

Regarding the quantitative analysis of dermal appendages (hair follicles and pilosebaceous glands), there was a significant difference among the groups ($P < 0.001$). The post hoc comparison revealed an increase of two-fold in dermal appendages in the 630/850 nm group when compared to control group ($P = 0.003$), an increase of two-fold in dermal appendages 630 nm versus 850 nm ($P = 0.007$), 1.5 times dermal appendages in 630/850 nm groups versus 630 nm group ($P = 0.01$), and three times more dermal appendages in the 630/850 nm groups versus 850 nm group ($P < 0.001$) (Fig. 2).

The quantitative analysis of vascular density (arterioles) also revealed a significant difference among the groups ($P < 0.001$). The post hoc comparison showed a difference between the group control versus 630/850 nm ($P = 0.01$), 630 nm versus 630/850 nm ($P = 0.0002$), and 850 nm versus 630/850 nm ($P < 0.001$). The 630/850 nm group showed six times more arterioles than the control group (Fig. 2).

Picrosirius staining showed more fine collagen fibers in the LED groups compared to the control group (Fig. 3).

Analysis of Gene Expression (IL-10, TNF-alpha, VEGF-a, MMP-9)

When comparing all the groups, there was no difference among them regarding the level of genic expression of VEGF-a and MMP-9. The level of genic expression of IL-10 showed significant differences ($P = 0.008$). When performing a pairwise comparison, there was difference between control and LED-630 nm ($P = 0.03$), LED-850 nm ($P = 0.005$), and LED-630 + 850 nm ($P = 0.0005$). This study
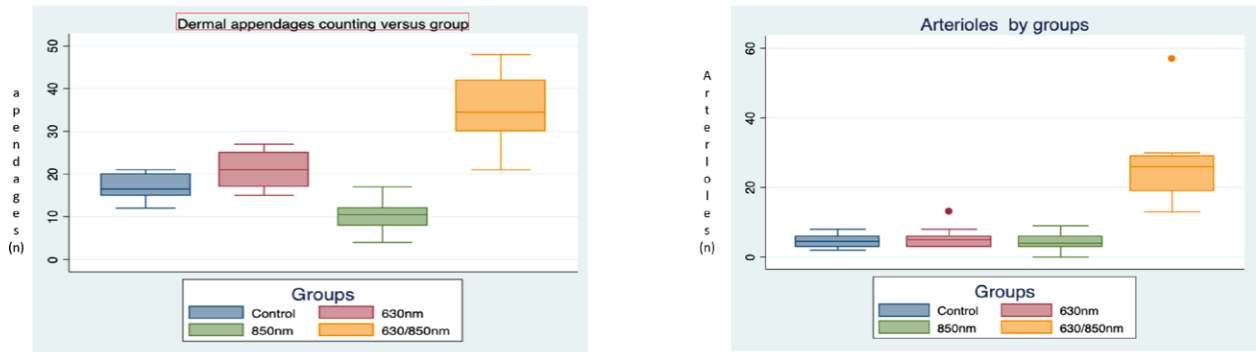
	Control Median (IQR) 95%CI	630nm Median (IQR) 95%CI	850nm Median (IQR) 95%CI	630/850nm Median (IQR) 95%CI
Dermal appendages	16.5 (15- 20) 14.4 – 18.9	21 (17-24) 17.9 -24.0	10.5 (8-12) 8.1 -13.3	34.5 (30-42) 1.1 – 1.8
Arterioles	4.5 (3-8) 3.2 – 5.8	5 (3-6) 3.1 – 7.6	4 (3-6) 1.9 – 5.8	26 (19-29) 6.4 – 13.8

Fig. 2. Graphic with histological element analysis (inflammatory cells, arterioles, and dermal appendages by groups: control group, 850 nm groups, 630 nm group, and 850 + 630 nm group).

Fig. 3. Picrosirius staining by groups (control group and LED group). The control group showed more fibrous collagen structure; however, all the laser groups showed a better organized and thin collagen structure.

also showed a decrease of 10-fold between LED-630 nm and LED-630+850nm (*P* = 0.02) (Fig. 4).

This study showed a difference regarding the level of genic expression of TNF-alpha (*P* = 0.02). A post hoc test showed a decrease of 12-fold between control and LED-630 nm (*P* = 0.006) and LED-850 nm (*P* = 0.002) (Fig. 5).

DISCUSSION

In this work, we developed and tested PBM therapy/PBM equipment that applies two different wavelengths and allows a combined wavelength therapy. The macroscopic analysis (skin radiodermatitis symptoms) showed a clinical benefit in all the groups treated with PBM.

In this sense, DeLand et al[13] analyzed the effect of using the PBM 590 nm (0.15 J/cm² twice a week) on radiodermatitis breast cancer patients. The findings showed a benefit of PBM in treating radiodermatitis. In agreement with these findings, the DERMIS[9] and TRANSDERMIS studies[13] showed a beneficial effect in PBM treatment (range from 808 to 905 nm, 0.15 J/cm², twice a week) in patients submitted to mastectomy and presenting radiodermatitis.[14]

The histological examination showed a beneficial effect of the LED treatment over the controls (no treatment). The association of 630+850 nm wavelengths induced higher vascular density and dermal appendage density. These findings suggested increasing cell division and cell migration from the basal layer of the epidermis. Therefore, this procedure shows a promising potential for radiodermatitis treatment. It probably increases the speed of epithelialization of the lesion. Park et al[15] tested two wavelengths (630 nm and 833 nm separately) in a mouse radiodermatitis model. They found a regenerative effect of LED treatment in the radiodermatitis region but no difference between 630 nm and 833 nm wavelengths in a mouse model.

Also, our group analyzed inflammatory, endothelial, and collagen interleukins regarding gene expression. Interestingly, our equipment showed a less inflammatory response, but we could not observe any significant changes in endothelial biomarkers.

PBM activates factors that increase gene expression related to collagen synthesis, cell migration and proliferation, antiapoptotic proteins, and antioxidant enzymes compared to literature data.[16,17] However, the certainty of the evidence is very low. In our study, we did not show any difference in fibrosis. Still, Dang et al[18] showed in an animal model study (young rats) that the 800 nm laser induced skin new collagen expression, thus improving skin structure. This agrees with other studies, also using experimental models, that showed that the PBM with Ga–As laser reduced histological abnormalities.[19]

Based on scientific data, our group adopted the wavelength ranges described in the literature.[7–10] In addition, according to the potential depth of light, we hypothesized the association of 630 nm (2–3 mm) and 850 nm (5–10 mm).[20]

According to literature data, photomodulation pieces of equipment show advantages, such as a noninvasive, low-cost therapeutical alternative. Based on these results, our group built a human prototype to analyze the effect of these wavelengths in human being trial (phase 2).

Moreover, there are still questions regarding the effect of photomodulation in cancer cells. Some authors analyze the impact of PBM stimulating cancer cells. In another way, some authors investigated the effect of PBM associated with chemotherapy as a coadjuvant oncologic treatment. Based on these contradictory results, new randomized clinical trials are mandatory to answer these essential questions.[21,22]

This study has limitations, such as the small sample size and the animal model choice. The rats showed some anatomical and histological specificities. The murine epidermal/dermal structure differs significantly from the human structure. Nevertheless, we can translate some findings to guide our future investigations.
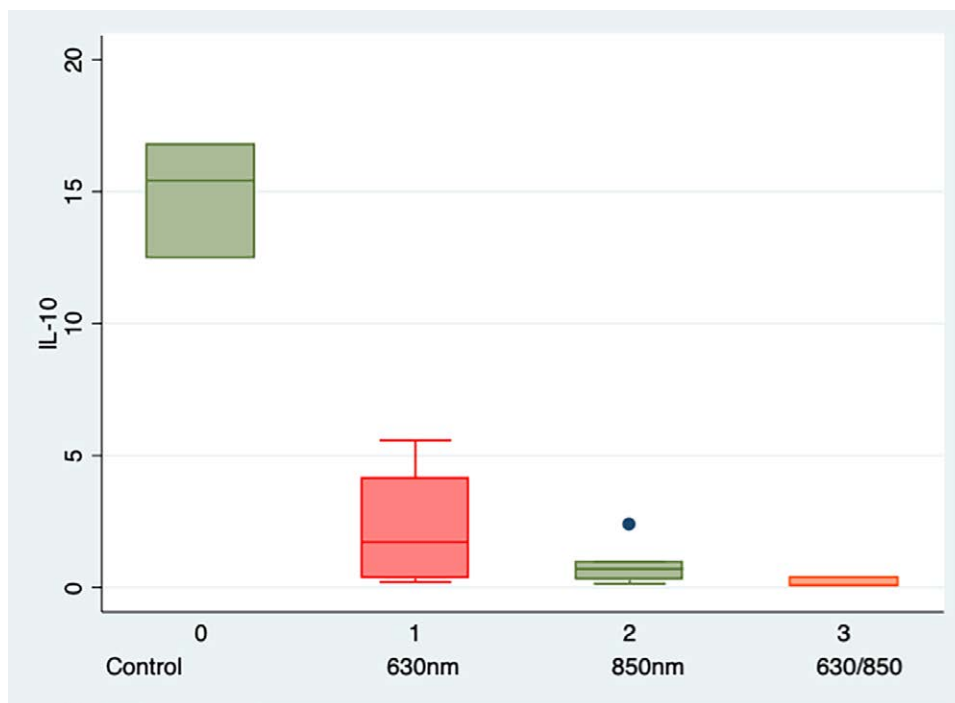
Fig. 4. IL-10 gene expression levels by different wavelength groups (control group, 850 nm groups, 630 nm group, and 850 + 630 nm group).
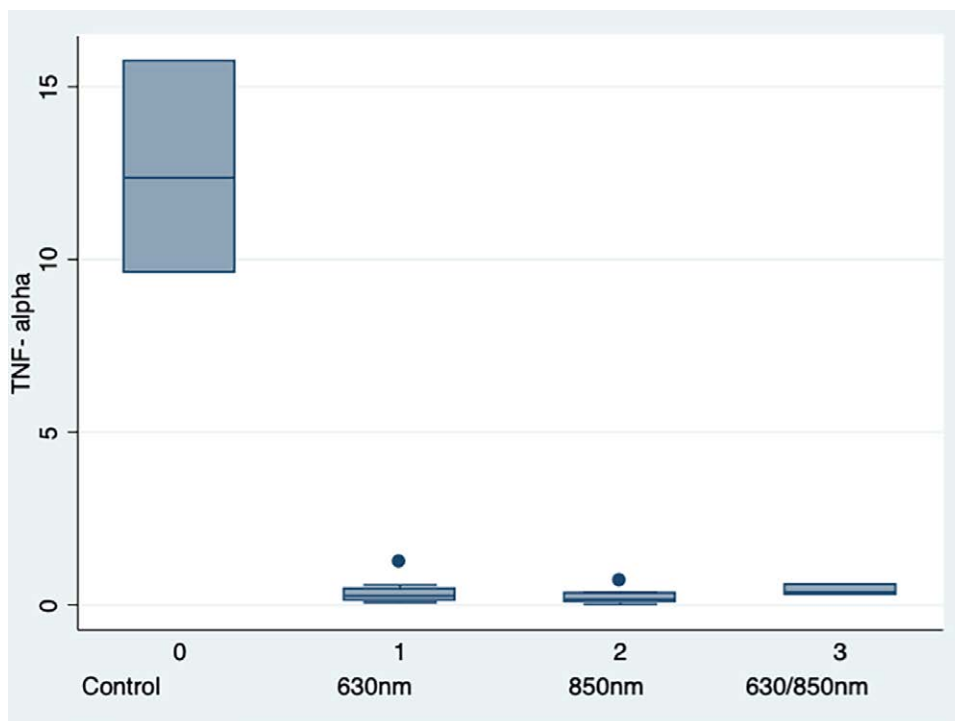

Fig. 5. TNF-alpha gene expression levels by different wavelength groups (control group, 850 nm groups, 630 nm group, and 850 + 630 nm group).

CONCLUSIONS

This study suggested that PBM therapy improves radio-dermatitis lesions in an animal model. More studies need to be done to prove cause effect.

Cristina Pires Camargo, MD, PhD
Universidade de São Paulo
Av Dr Arnaldo, 455 room 1363
CEP 01243-906
SãoPaulo, Brazil
E-mail: cristinacamargo@usp.br

REFERENCES

1. Bray FN, Simmons BJ, Wolfson AH, et al. Acute and chronic cutaneous reactions to ionizing radiation therapy. *Dermatol Ther (Heidelb)*. 2016;6:185–206.
2. Gianfaldoni S, Gianfaldoni R, Wollina U, et al. An overview on radiotherapy: from its history to its current applications in dermatology. *Open Access Maced J Med Sci*. 2017;5:521–525.
3. Chan RJ, Webster J, Chung B, et al. Prevention and treatment of acute radiation-induced skin reactions: a systematic review and meta-analysis of randomized controlled trials. *BMC Cancer*. 2014;14:53.
4. Schneider F, Pedrolo E, Lind J, et al. Prevenção e tratamento de radiodermatite: uma revisão integrativa. *Cogitare Enfermagem*. 2013;18:579–586.
5. Hegedus F, Mathew LM, Schwartz RA. Radiation dermatitis: an overview. *Int J Dermatol*. 2017;56:909–914.
6. Kole AJ, Kole L, Moran MS. Acute radiation dermatitis in breast cancer patients: challenges and solutions. *Breast Cancer (Dove Med Press)*. 2017;9:313–323.
7. Leventhal J, Young MR. Radiation dermatitis: recognition, prevention, and management. *Oncology (Williston Park)*. 2017;31:885–899.
8. de Freitas LF, Hamblin MR. Proposed mechanisms of photobiomodulation or low-level light therapy. *IEEE J Sel Top Quantum Electron*. 2016;22:348–364.
9. Robijns J, Lodewijckx J, Mebis J. Photobiomodulation therapy for acute radiodermatitis. *Curr Opin Oncol*. 2019;31:291–298.
10. Strouthos I, Chatzikonstantinou G, Tselis N, et al. Photobiomodulation therapy for the management of radiation-induced dermatitis: a single-institution experience of adjuvant radiotherapy in breast cancer patients after breast conserving surgery. *Strahlenther Onkol*. 2017;193:491–498.
11. Zlatko S; European Medical Laser Association. Lasers in medicine and dentistry: basic science and up-to-date clinical application of low energy-level laser therapy. *LLLT*. 2000. Available at https://waltpbm.org/lasers-in-medicine-and-dentistry/
12. Cox JD, Stetz JA, Pajak TF. Toxicity criteria of the Radiation Therapy Oncology Group (RTOG) and the European Organization for Research and Treatment of Cancer (EORTC). *Int J Radiat Oncol Biol Phys*. 1995;31:1341–1346.
13. DeLand MM, Weiss RA, McDaniel DH, et al. Treatment of radiation-induced dermatitis with light-emitting diode (LED) photomodulation. *Lasers Surg Med*. 2007;39:164–168.
14. Robijns J, Censabella S, Claes S, et al. Prevention of acute radiodermatitis by photobiomodulation: a randomized, placebo-controlled trial in breast cancer patients (TRANSDERMIS trial). *Lasers Surg Med*. 2018;50:763–771.
15. Park JH, Byun HJ, Kim HJ, et al. Effect of photobiomodulation therapy on radiodermatitis in a mouse model: an experimental animal study. *Lasers Med Sci*. 2021;36:843–853.
16. Censabella S, Claes S, Robijns J, et al. Photobiomodulation for the management of radiation dermatitis: the DERMIS trial, a pilot study of MLS laser therapy in breast cancer patients. *Support Care Cancer*. 2016;24:3925–3933.
17. Karu TI. Special issue papers. Photobiological fundamentals of low-power laser therapy. *IEEE J Quantum Electron*. 1987;23:1703–1717.
18. Dang Y, Liu B, Liu L, et al. The 800-nm diode laser irradiation induces skin collagen synthesis by stimulating TGF-β/Smad signaling pathway. *Lasers Med Sci*. 2011;26:837–843.
19. Fillipin LI, Mauriz JL, Vedovelli K, et al. Low-level laser therapy (LLLT) prevents oxidative stress and reduces fibrosis in rat traumatized Achilles tendon. *Lasers Surg Med*. 2005;37:293–300.
20. Opel DR, Hagstrom E, Pace AK, et al. Light-emitting diodes: a brief review and clinical experience. *J Clin Aesthet Dermatol*. 2015;8:36.
21. Hamblin MR, Nelson ST, Strahan JR. Photobiomodulation and cancer: what is the truth? *Photomed Laser Surg*. 2018;36:241–245.
22. Klausner G, Bensadoun RJ, Champion A, et al. État de l'art de la photobiomodulation dans la prise en charge des effets secondaires de la radiothérapie: indications et niveaux de preuve [State of art of photobiomodulation in the management of radiotherapy adverse events: indications and level of evidence]. *Cancer Radiother*. 2021;25:584–592.